CHARGE TRANSFER DURING INDIVIDUAL COLLISIONS IN ICE GROWING BY RIMING

Eldo E. Avila and Giorgio M. Caranti

Facultad de Matemática Astronomía y Física, Universidad Nacional de Córdoba

Laprida 854, 5000 Córdoba, Argentina.

ABSTRACT

The charging of a target growing by riming in a wind tunnel has been studied in the temperature range of (-10, -18°C). For each temperature, charge transfers of both signs are observed and according to the environmental conditions one of them prevails. The charge is more positive as the liquid water concentration is increased at any particular temperature. It is found that even at the low impact velocities used (5 m/s) there is abundant evidence of fragmentation following the collision.

Introduction

Many experimental studies about charge transfer while the target in a wind tunnel or the rimer in a cloud chamber grow by riming involve multiple collisions (Reynolds et al, 1957, Takahashi 1978, Jayaratne et al 1983). This made dificult to establish the mechanism or mechanisms of charging. The measured electrical current in these experiments were the result of many collisions and therefore a null result could simply be due to equal numbers of positive and negative charge transfers.

Jayaratne et al (1983) observed while working on multiple collisions that the charge current dropped significantly when the steam supply was cutoff. This result is subject to different interpretations. It should be noted that the cristals would grow at expenses of the droplets which dissipate very soon.

Recently, there have been attempts of measuring the charge transfer when only very few crystals impacted at a given time (low frequency of collisions) in order to infer the charge transferred per collision. Kumar and Saunders (1989) measured the charge transfer between ice crystals and a previously rimed target at low frequency. The cloud droplets were also drawn past the target so it is expected that some riming was simultaneous to the charging. Unfortunately, there was not a quantification of the amount of riming the target was undergoing.

There are a number of mechanism being proposed as responsible for the charge transfer. Among them the contact potential (Buser and Aufdermaur 1977), the liquid like layer (Baker and Dash 1989), the presence of charged dislocations on the surface (Keith and Saunders 1989). Each mechanism seems to explain part of the observations.

Baker et al (1987) working on multiple collisions experiments arrived to the

conclusion that the sign depended on the relative rate of growth of the interacting particles, the fastest growing particle would get positive charge. Keith and Saunders (1990) also measuring multiple collisions arrived at a different conclusion and they suggest that charged dislocations on the surface of the interacting particles are responsible for the observed transfers. This process would also yield only one sign for a given set of conditions. Nevertheless, there is evidence that under the same target surface and particle conditions it is possible to obtain a mixture of signs. In fact, Avila et al (1988), measured single collisions and found a that almost invariably there was not a single sign.

Caranti et al 1991 studied individual collisions of ice crystals with a target growing by vapor deposition. They showed direct evidence that at least on a target subject to these conditions the breaking of protuberances on the surface could be associated with the charge deposited on the target. This work is extended here to riming and further support to the physical model presented in that work is given.

Experimental Set up

The arrangement was basically the same as in Caranti et al 1991. The experiments were carried out in a wind tunnel placed inside a cold room. On top of which the drop generator [*Abbott and Cannon* 1972] was installed. This generator produces water drops of a uniform size which can be selected in a relatively wide range. Both the repetition rate and the charge placed on the drops can be controlled. In the present experiment only sizes close to 100 μm were used.Each drop formed at laboratory temperature is frozen as it falls though a liquid air cooled region of the tunnel. After freezing the particle has a free fall of more than 50 cm that allows for thermalization. There is an acceleration zone where cold room air

enters the tunnel and drags the particle with it to collide the target at the wanted speed. In this reported work the velocity was 5 m/s.

Figure 1 shows the working section of the tunnel. Twelve centimeters upstream from the target there is an induction ring sensing the charge on the frozen drops. The target is a copper cylinder 4 mm in diameter connected on an end with a sensitive charge amplifier capable of detecting charges larger than 2 fC. The amplifier has associated with it a time constant of about 100 ms. Eight centimeters downtream from the target there is another induction ring with the purpose of detecting the products of the collisions. The two rings were electrically interconnected and to another amplifier. Since the total time of pasage of a particle at 5 m/s between the two rings would be 40 ms and the repetition rate about 1 s there is no aliasing.

Unlike the previous experiment and due to the added complexity the cloud drawn past the tunnel impose in this case the signals from the target and from the rings were not added. This helped to distinguish better the origin of pulses that looked like transferences to the target but they were actually transferences to the rings. The noise levels were also kept at manageable levels by this arrangement.

So each charge transfer event has several pulses associated with it. The first pulse comes from the upstream induction ring and is recorded on the ring channel. The amplitude of this pulse is proportional to the initial charge that the particle brings and its duration is of approximately 4 ms, depending on the velocity. The second pulse recorded on the target channel is separated about 24 ms from the first originates in the target and it is related both to the induction of the initial charge of the particle and to the transfer itself. This latter event is distinguished from a near miss because of the mentioned 100 ms decay. Finally, any byproducts

of the collision namely the original particle and/or fragments if they are produced are detected at the second ring and recorded on the ring channel . The signals are both magnetically recorded for later process and measured in real time using a digital oscilloscope (Tektronik 2020). As before the shape of each pulse contains a welth of information and therefore it is better to analize them on a one by one basis.

The cloud was generated outside the cold room by boiling water. The water vapor was conducted inside by several tubes. The first brass section at the outside was cooled by evaporation. Next, a corrugated plastic section entered the cold room followed by a 1 m brass section that ensured thermalization. The cloud entered a small chamber that sorrounded the tunnel and was drawn into the tunnel through two symetrically placed tubes positioned between thc first induction ring and the target. This disposition ensured a minimum flow perturbation and therefore no significant increase in the number of particles that miss the target was found.

Ultrasonic generators were also used but in the end steam was preferred because it lacked appreciable charge density resulting in a clearer signal.

Experiments and Results

The charge transfer was measured in individual collisions between 100 μm ice particles at 5 m/s and an target undergoing simultaneous riming.

The measurements were carried out for ambient temperatures (T_a) between -10 and -18 ^oC. The ambient relative humidity was lower than saturation and within the range of 60 to 80 % over ice according to the cold room cycle. This made necessary monitoring the cloud liquid water concentration during each run

in order to take into account the cloud dilution. Typical effective values were around 0.5 g/m^3.

The determination of the liquid water concentration (LWC) was done by weighting the mass of water collected by the target during a given time. LWC is then calculated dividing the mass by the corresponding time interval times the cross sectional area of the target and the air velocity. This procedure of course assumes an unity collection efficiency and therefore the term "effective" LWC.

Figure 2 shows typical charge transfer pulses. The upper trace represent the signal coming from both rings simultaneously. The lower trace shows the signal originated in the target. In general it is possible to distinguish the rebounding initial particle from the fragments because of their different masses. Their respective downstream ring pulses can be resolved due to the different times they take to attain the air velocity, resulting in unequal time delays for the downstream ring passage. In Figure 2a the positive charge transfer is clearly seen in the target signal after the passage of a particle through the first induction ring. The ring signal also shows the postimpact passage of two particles through the second ring. Figure 2b shows an interesting case of probable trapping of the impacting particle but with the emision of a fragment. A case of negative charge transfer is seen in Figure 2c. In a similar fashion as in Figure 2a there are fragments detached from the target showing that fracture occurs irrespective of the sign of the charge transfer. In all cases a check of the conservation of charge is made; assuming the target is initially uncharged the sum of all charges (target and downstream ring) after the collision should be equals to that of the incomming particle before the impact. This ensures that possible interactions of the rebounding particles with the tunnel walls do not affect the interpretation of results.

The initial charge on the impacting particle was not taken into account in previous work mainly because the charge transfer experiments involved smooth ice targets. In the present case the surface of the target is so uneven that there is a greater possibility of partial trapping in which the incoming particle spends more time in contact with the target maybe transferring its initial charge. Nevertheless, these cases are easily detected from the oscilloscope pulses.

Figure 3 shows the histograms for three runs with an effective LWC of 0.2 g/m^3 at different temperatures ($-10, -15$ and -18^oC). There is a mixture of signs with a dominance of the positive pulses in all three runs. Figure 4 shows data taken at slightly higher LWCs. The data corresponding to -12^oC was taken at 0.3 g/m^3 while the data for -15 and -18^oC was taken at 0.5 g/m^3.

A first observation from these Figures is that as the LWC is increased it is necessary decrease the temperature in order to obtain negative charge transfers. The charge magnitudes are comprised in the range $\pm$ 50 fC in accordance with the observations of Gaskell and Illingworth (1980). From a statistical point of view it is important to mention that about 50% of recorded events are observed to produce fragments. Moreover, there is a proportion of events similar to that illustrated in Figure 2b which cannot be categorize with total certainty as fractures but they have a high probability of being so, bringing the total to about 80%.

Discussion

Caranti et al (1991) noted that for a smooth ice target just placed into the wind tunnel the charging was different from that of a target that had the opportunity to grow new ice on it. They observed a mixture of signs during the initial growth from the vapor and suggested that the presence of both signs could be

associated to two different kind of surfaces.

They also suggested that the transfer of negative charge observed when the ice particles collide with an evaporating ice substrate could be caused by a contact potential difference between the interacting ice surfaces. In fact, *Caranti and Illingworth* [1983] found a relatively strong contact potential change when ice was rimed or was subjected to rapid freezing. A similar change could not be associated to vapour growth, which prompted Caranti et al (1991) to suggest that the positive transfers were probably caused by the fragmentation of dendrites from the surface of the growing particle.

The phenomenological model they proposed was based on the fact that significant temperature gradients are created when a particle grows. Fracture under these gradients can be a source of charge for the measured transfers. In that work it is shown that the sign of the charge transfer follows the sign of temperature gradient. When the surface was growing by vapor deposition the charge left on the target was positive.

The droplets landing on the target form structures or piling ups as long as the their influx does not go over the limit of wet growth. This piling ups are inherently fragile and could break under impact (or even without). During this accretion process the temperature gradients are caused by the release of freezing latent heat. The heat released has also the overall effect of warming up the the whole accretion. Now, a droplet landing on top of a pile will heat up the outer end of it, creating a outward pointing temperature gradient ∇T. Neighbouring piles will also be heated but by vapor deposition since the freezing drop is a strong vapor source. On the other hand the piles away from a freezing drop and evaporating will have an inward pointing ∇T.

The fraction of piles having a given sign of the gradient will be related to the droplet influx and therefore to the product of LWC and the air velocity. The other parameter, this fraction of piles is related to is the temperature. As the temperature is lowered the time it takes for a droplet to freeze diminishes and on average its influence on the sorroundings also decreases. The probability a collision results in the fracture of a pile with a given ∇T will be related to this fraction.

The results illustrated in Figures 3 and 4 are consistent with the above description. In fact, the fraction of positive pulses at a given T is clearly proportional on the LWC (all runs were at the same air velocity). So much that in certain runs there were only positive pulses. The influence of the temperature is also seen in those figures.

Conclusion

Several researchers working on multiple collisions (eg. Kumar and Saunders 1989) argue that given a particular set of environmental conditions the charge transfers would have only one sign. The results presented here show that most of the time there is a mixture of signs and that the environment influence only which one is the dominant.

The fracture charging is observed to work in a wide range of temperatures and for impact velocities relevant to cloud physics.

It is important to stress the large proportion of collisions followed by fracture observed. There is evidence that the size of the fragments will allow them to grow from the vapor as any other ice crystal in the cloud. Therefore this is a viable multiplication mechanism.

References

Abbott, C. E., and T. W. Cannon, A droplet generator with electronic control of size, production rate, and charge, *Rev. Sci. Instrum.*, *43*, 1313–1317, 1972.

Avila, E.E., G.M.Caranti and M.A. Lamfri, Charge reversal in individual ice-ice collisions, *Proc.* 8^{th} *International conference on atmospheric electricity* 245–250, Uppsala, Sweden, 1988.

Baker B., M.B. Baker, E.R. Jayaratne, J. Latham and C.P.R. Saunders, The influence of diffusional growth rates on the charge transfer accompanying rebounding collisions between ice crystals and soft hailstones. *Q. J. R. Meteorol. Soc.*, *113*, 1193-1215, 1987.

Baker M.B. and Dash J.G. Charge transfer in thunderstorm and the surface melting of ice *J. Crystal Growth, 97*, 770-776, 1989.

Buser O. and A.N. Aufdermaur, Electrification by colDision ofice particles on ice or metal target *in Electrical processes in the atmospheres*, Steinkopf Darmstadt, 1977.

Caranti J.M., E.E. Avila and M.A. Ré, Charge transfer during individual collisions in ice growing from vapor deposition. *J. Geoph. Res.* in press. 1991.

Caranti J.M. and A.J. Illingworth, The contact potential of rimed ice. *J. Phys. Chem. 87*, 4125, 1983.

Gaskell W. and A.J. Illingworth, Charge transfer accompanying individual collisions between ice particles and its role in thunderstorm electrification. *Q. J. Roy. Met. Soc. 106*, 841–854, 1980.

Jayaratne E.R., C.P.R. Saunders and J. Hallett, Laboratory studies of the charging of soft hail during ice crystals interactions. *Quart. J. Roy. Met. Soc. 109*, 609–630, 1983.

Keith W.D. and C.P.R. Saunders, Charge transfer during multiple large ice crystal interactions with a riming target. *J. Gheoph. Res. 94*, 13103-13106, 1989.

Keith W.D. and C.P.R. Saunders, Further laboratory studies of the charging of graupel during ice crystals interactions. *Atm. Res. 25*, 445–464, 1990.

Kumar P.P. and C.P.R. Saunders, Charger transfer during single crystal interaction with a rimed target. *J. Gheoph. Res. 94*, 13099-13102, 1989.

Reynolds S. E., M. Brook and Mary Foulks Gourley, Thunderstorm charge separation . *J. Meteor. 14*, 426–436, 1957.

Takahashi T., Riming electrification as a charge generation mechanism in thunderstorms. *J. Atmos. Sci. 35*, 1536–1548, 1978.

Figure Captions

Figure 1. Left: vertical cross section of the working stage of the wind tunnel. The target is a cylindrical rod. The arrow indicates the flow direction. Right: horizontal cross section along the A-A line. The steam is generated outside the cold room and is thermalized before entering this stage.

Figure 2. Typical events with particles of 100 μm impacting at 5 m/s. Top trace: added signals from the two induction rings. Bottom trace: the target signal. (See text for description)

Figure 3. Charge transfer histograms taken at three temperatures. The effective liquid water concentration LWC was 0.2 g/m^3.

Figure 4. The same as in Figure 3 but for LWC 0.5 g/m^3.

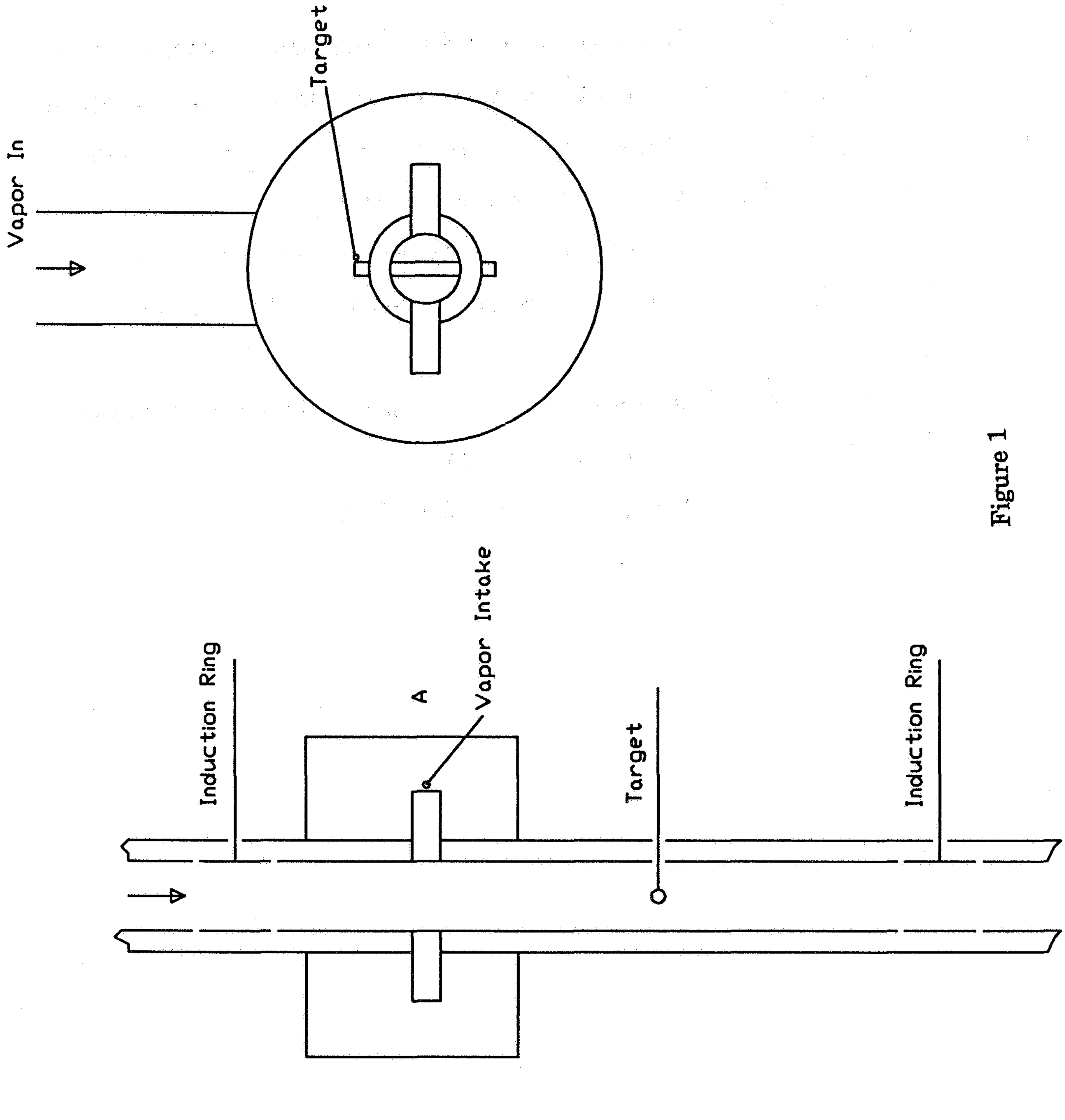
Vapor In
Target
Induction Ring
A
Vapor Intake
Target
Induction Ring

Figure 1

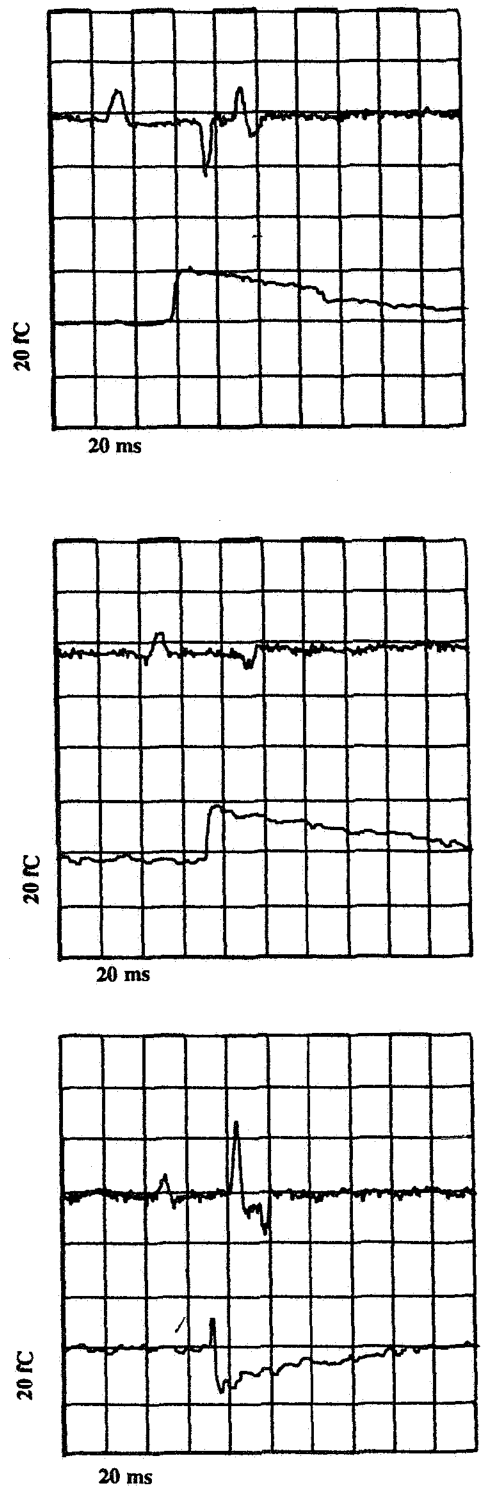

Figure 2

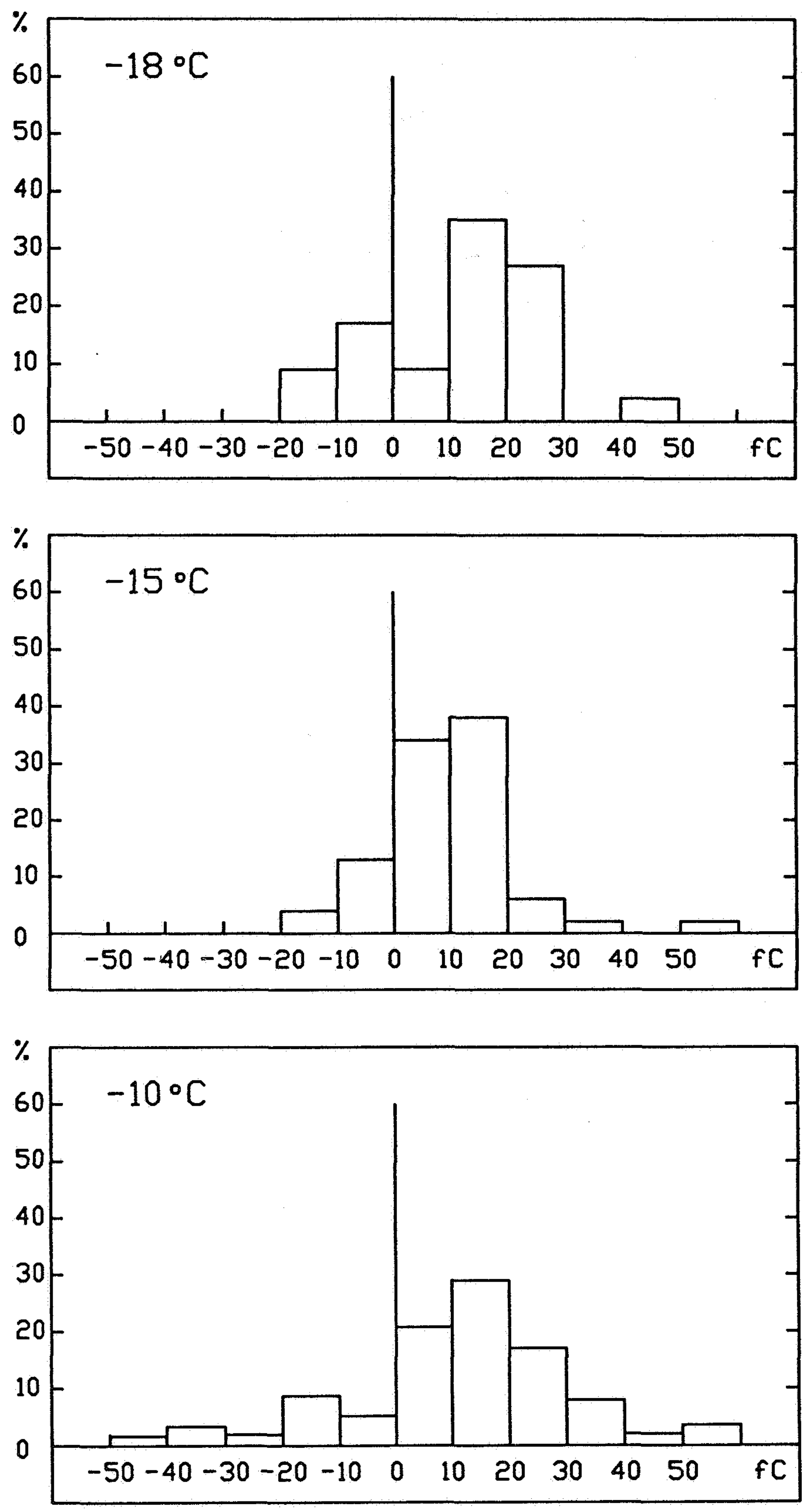

%
-18 °C
60
50
40
30
20
10
0
-50 -40 -30 -20 -10 0 10 20 30 40 50 fC
%
-15 °C
60
50
40
30
20
10
0
-50 -40 -30 -20 -10 0 10 20 30 40 50 fC
%
-10 °C
60
50
40
30
20
10
0
-50 -40 -30 -20 -10 0 10 20 30 40 50 fC

Figure 3